

NCC 1-55 (2)

NASA

1N-25-CR

127097

P-50

The Vibrational Spectrum of H_2O_3 : An *ab initio* Investigation.

Charles F. Jackels
Department of Chemistry
Box 7486
Wake Forest University
Winston-Salem, North Carolina 27109

(NASA-CR-190968) THE VIBRATIONAL
SPECTRUM OF H_2O_3 : AN AB INITIO
INVESTIGATION (Wake Forest Univ.)
50 p

N93-12935

Unclas

G3/25 0127097



ABSTRACT

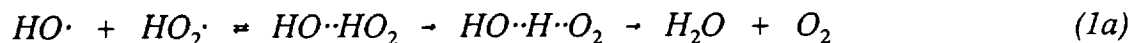
Theoretically determined frequencies and absorption intensities are reported for the vibrational spectrum of the covalent HOOOH and hydrogen bonded HO...HOO intermediates that may form in the reaction of the hydroxyl and hydroperoxyl radicals. Basis sets of DZP quality, augmented by diffuse and second sets of polarization functions have been used with CASSCF wave functions. The calculated harmonic vibrational frequencies of HOOOH have been corrected with empirical factors and presented in the form of a "stick" spectrum. The oxygen backbone vibrations, predicted to occur at 519, 760, and 870 cm^{-1} , are well separated from most interferences, and may be the most useful for the species' identification. In the case of the hydrogen bonded isomer, emphasis has been placed upon prediction of the *shifts* in the intramolecular vibrational frequencies that take place upon formation of the complex. In particular, the HO stretch and HOO bend of HO₂ are predicted to have shifts of -59 and 53 cm^{-1} , respectively, which should facilitate their identification. It is also noted that the antisymmetric stretching frequency of the oxygen backbone in HOOOH exhibits a strong sensitivity to the degree of electron correlation, such as has been previously observed for the same mode in ozone.

I. INTRODUCTION

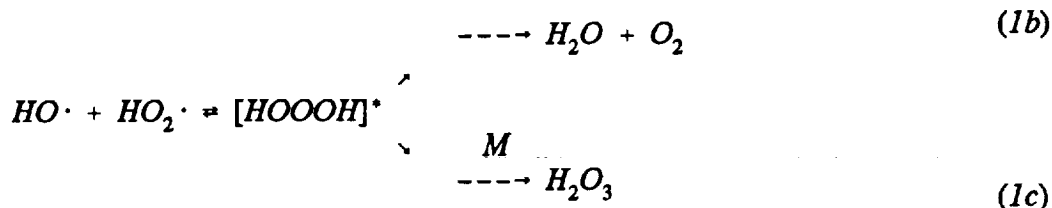
The reaction of the hydroxyl and hydroperoxyl radicals to produce water and oxygen



has received a great deal of experimental and theoretical attention in recent years. In its own right, this reaction plays an important role in determining hydroxyl radical concentrations in models of atmospheric and combustion chemistry. It is also of interest as a prototype for reactions involving more complex radical species. The bimolecular rate constant for reaction (1) was found to be quite large. Early measurements of it exhibited an apparent pressure dependence, with k_1 increasing from about $0.1-0.5 \times 10^{-10} \text{ cm}^3\text{s}^{-1}\text{molecule}^{-1}$;^{1,2,3,4} to about $1-2 \times 10^{-10} \text{ cm}^3\text{s}^{-1}\text{molecule}^{-1}$;^{5,6,7,8,9,10} as the total pressure was increased from a few torr to one atmosphere. The initial investigation of the temperature dependence¹¹ of k_1 yielded an estimate of $E_a/R = -416 \pm 86 \text{ K}$. The large value of k_1 coupled with its apparent pressure dependence and negative activation energy generated a great deal of interest^{12,13,14,15} in the detailed mechanism of reaction (1), with considerable debate over whether it followed a direct abstraction mechanism (possibly *via* a hydrogen bonded intermediate),



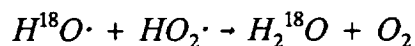
proceeded *via* a stabilizable covalent intermediate,



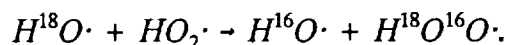
or followed both pathways.

Recent studies^{16,17} have indicated that the low and high pressure measurements of k_1 may agree to within the precision of the data, and the apparent pressure dependence is currently explained in terms of experimental uncertainties and systematic errors in the earlier data. The temperature dependence of reaction (1) has also been reinvestigated¹⁶, indicating a smaller value of $E_a/R = -250 \pm 50$ K. The rate constant value at 298 K currently recommended by the NASA panel¹⁸ for use in atmospheric modeling ($1.1 \times 10^{-10} \text{ cm}^3 \text{ s}^{-1} \text{ molecule}^{-1}$) has no pressure dependence and a temperature dependence given as $E_a/R = -250 \pm 200$ K.

Two isotopic substitution studies have been carried out to elucidate the mechanism of reaction (1). Kurylo *et al.*⁷ studied the $H^{18}O \cdot + HO_2 \cdot$ reaction at high pressure (1 atm of SF_6) and concluded that formation of the products did not proceed *via* the HOOOH intermediate of reaction (1b), because an insufficient amount of the $^{16}O^{18}O$ product was found. A low pressure $H^{18}O$ study by Dransfeld and Wagner¹³ found the rate for the reaction



to be roughly equal to that of the exchange reaction



These authors attributed the formation of water and molecular oxygen to mechanism

(1a) and indicated that the formation of the HOOOH intermediate resulted in dissociation to reactants rather than stabilization under their conditions. The results of Kurylo *et al.*⁷ were reconciled with their own by suggesting that the stabilization path (1c) completely dominated the isotope exchange dissociation under the conditions of Ref.7 (1 atm of SF₆), thus accounting for the fact that very little ¹⁶O¹⁸O had been observed.

These mechanistic studies, combined with theoretical results and the knowledge that the pressure dependence is probably not strong, has encouraged analysis of the mechanism of reaction (1) in terms of the direct abstraction pathway.^{15,17,19,20} The existence of a potential energy well corresponding to a weakly bound hydrogen bonded intermediate, as in reaction (1a), can be used to account for the negative temperature dependence of reaction (1).

Early theoretical work on this system focused on the ground state potential energy surface of the HOOOH intermediate. Work from this laboratory²¹ and others^{15,19,20} has provided stability estimates of both the covalently bonded and hydrogen bonded intermediates. The earliest work²² that included electron correlation paid particular attention to the potential surface for torsional motion about the O-O single bonds in HOOOH. Recent computational studies^{15,19,20} have characterized not only the energy minima of the intermediates, but also transition states on some of the low lying surfaces. Gonzalez *et al.*^{19,20} have employed *ab initio* potential surfaces (¹A, ³A', and ³A") in combination with rate theory calculations to study both the temperature and pressure dependence of reaction (1). Their results generally are in agreement with the experimental interpretations: product formation at normal conditions is due almost entirely to reaction (1a) on the triplet surfaces; the temperature dependence of reaction

(1a) can be modeled in reasonable agreement with experiment; the pressure dependence due to reaction (1c) will not be important with helium as bath gas below about 5 atmospheres; and, due to a significant activation energy, rearrangement of HOOOH on the 1A surface to form the overall products, reaction (1b), will not be important except at high temperatures.

It is expected that reaction (1) will continue to receive both theoretical and experimental attention and that the nature of the intermediates will remain central to these investigations. While the present evidence indicates¹⁹ that in helium the HOOOH intermediate is not stabilized except at pressures exceeding five atmospheres, the suggestion¹³ stabilization is dominant over unreactive dissociation in one atmosphere of SF₆ raises questions about the importance of channel (1c) in atmospheric and combustion environments. In comparing the ratio of k_{1a} to the rate constant for formation of [HOOOH]^{*}, the authors of Ref. 20 find a 6-fold disagreement between value deduced from the isotope studies and that arising from the rate theory calculations. In further studies at high pressure it would be very interesting to probe directly for the presence of stabilized intermediates; the high pressure flow system recently developed by the Harvard group²³ is especially intriguing in this regard. Since Fourier transform infrared spectroscopy (FTIR) could be an effective detection method for any such intermediate, it would be useful to have in hand theoretical predictions of the vibrational absorption spectrum (frequencies and intensities) for these intermediate species.

From a theoretical point of view, the vibrational frequencies of HOOOH are interesting because of the molecule's similarity to ozone. The magnitude and order of the calculated ozone vibrational frequencies is extremely sensitive to the level of theory

employed.²⁴ In that case the well known requirement to describe adequately the biradical character of the ground state²⁵ becomes entangled with other aspects of the electron correlation problem, and a clear understanding of the difficulty in describing the vibrational frequencies is not easily obtained. The 1A ground state of HOOOH has no biradical complications and is reasonably well described by a closed shell wave function, making examination of its -OOO- backbone modes with those of ozone quite interesting.

The present study reports the results of an *ab initio* quantum chemical determination of the vibrational frequencies and absorption intensities of both the covalently bonded HOOOH intermediate and the triplet ground state hydrogen-bonded HO---HO₂ species. Vibrational frequencies calculated using many-body perturbation theory methods have appeared in the literature for HOOOH, but the intensities have not been previously reported. Neither the vibrational frequencies nor the absorption intensities have been reported for the $^3A'$ ground state of the hydrogen-bonded complex, although the frequencies of the closely related $^3A''$ excited state minimum and transition state have been published.²⁰

II. COMPUTATIONAL METHOD

A. Basis Sets.

This study employed a polarized double-zeta (DZP) quality Cartesian Gaussian basis set consisting of Dunning's [4s2p|2s] contraction²⁶ of Huzinaga's (9s5p|4s) set.²⁷ A scale factor of $\zeta = 1.2$ was chosen for the hydrogen *s* functions, and polarization was provided by a set of *d* functions on oxygen (exponent, $\alpha = 0.85$) and a set of *p* functions on hydrogen (exponent, $\alpha = 1.0$). In some phases of the work the DZP basis was augmented by replacing the single set of *d* functions with a double set (exponents, $\alpha_1 = 0.425$, $\alpha_2 = 1.70$) and is denoted DZP(2d). When an *sp* set of diffuse functions was present on the oxygen atoms (exponent, $\alpha = 0.059$), the basis set notation is given as DZP(+) or DZP(2d,+). Because of program limitations, some of the many-body perturbation theory calculations were carried out with a split valence 6-31G** basis²⁸ that is of similar quality to the DZP basis.

B. Electronic Structure Calculations.

In general the SCF calculations reported here are of either closed- or open-shell spin restricted type, except that UHF calculations were utilized to define the orbital basis for the open-shell perturbation theory results. The MCSCF calculations used throughout this study are of the complete active space²⁹ (CASSCF) variety and utilize a density matrix driven algorithm.³⁰ The notation "MC[n,m]" will be used to designate an expansion that includes all possible configurations for *n* electrons in *m* molecular orbitals. Geometry optimization was performed using the algorithm of Baker.³¹ The many-body perturbation theory (MBPT) calculations were carried out at the second and fourth order (MP2 and MP4[SDTQ]) using the methodology of Pople and coworkers.³²

C. Vibrational Spectra.

The vibrational spectra were calculated in the "double harmonic" approximation³³ in which the potential surface is assumed to be quadratic and the electric dipole moment is assumed to vary linearly near the potential surface minimum. In most cases the second derivatives of the energy were calculated by numerical central differences of analytical energy gradients that had been determined at small displacements about equilibrium. In the case of SCF wave functions, the energy second derivatives were directly calculated by analytical methods, and in the MP4 case they were determined as second differences of energies at displaced geometries.

D. Computer Programs.

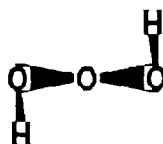
The MCSCF and SCF calculations were carried out using the North Dakota State version of the GAMESS³⁴ electronic structure package, and the MBPT calculations utilized the Gaussian 86/88/90 programs.³⁵ Computers used in this study included the Convex C1, the Sun Sparc 2, and the Cray YMP.

III. RESULTS AND DISCUSSION

A. The Covalent HOOOH Species.

1. *Equilibrium geometry*

The results of this study for the minimum energy conformation of the 1A ground state of the HOOOH molecule are reported in Table I, along with those previous results that employed correlated wave functions. The molecule displays C_2 symmetry at the energy minimum, and from the table it is noted that the bond lengths and angles are



HOOOH Covalent Intermediate

quite insensitive both to the level of the CAS treatment and to augmentation of the basis set. The active space of the MC[8,8] wave functions includes the eight sigma bonding electrons in the space of the four bonding and four antibonding molecular orbitals. The MC[14,11] wave functions include one nonbonding lone pair on each oxygen in the active space, giving an MCSCF expansion of 32,670 configuration spin functions at unsymmetric (C_1) conformations.

In general with basis sets of this quality, it is expected that experimental bond length would be bracketed by the SCF and CASSCF level results, and the experimental value of R_{OH} should lie in the range 0.965-0.970 Å. However, the OO bond distance merits special attention because the change from the RHF to CASSCF results is unusually large (+0.09 Å). To assist in evaluation of these results, we carried out

calculations using the same basis set and comparable electron correlation treatments on hydrogen peroxide, which has a similar O-O single bond. In that case, the optimum O-O bond length was found to increase from 1.391 to 1.487 Å as the treatment progressed from RHF to MC[10,8], which is comparable to the progression from RHF to MC[14,11] for H₂O₃. This R_{OO} value of 1.487 Å is about 0.03 Å longer than the most accurate H₂O₂ theoretical³⁶ and experimental³⁷ values, 1.462 and 1.464 Å, respectively. By analogy, it is expected that a more accurate treatment of H₂O₃ including dynamic electron correlation would reduce the value of R_{OO} to about 1.43 Å, which is predicted to be quite close to the experimental value.

Based upon similar calculations for H₂O₂ and H₂O, the HOO bond angle from our MC[14,11] calculations are expected to be reasonably accurate, with the experimental result predicted to be several tenths of degree larger. The OOO angle is expected to be sensitive to the correlation treatment of the oxygen lone pairs, and the results in Table I show that it varies considerably as the MCSCF active space is enlarged. However, the overall variation in Θ_{OOO} is only 2.5°, so we predict that the MC[14,11] values are probably accurate to within $\pm 1^\circ$. The dihedral angle is harder to predict because of the flatness of the torsional potential and may be in error by several degrees.

2. *Vibrational frequencies*

The harmonic vibrational frequencies calculated for the covalent H₂O₃ species are presented in Table II, along with the available experimental observations³⁸. The subscripts used to index the normal modes do not follow the sequence in Ref. 38. Rather, they are assigned by placing the normal modes in order of increasing frequency as determined at the RHF/DZP level. Examination of the normal modes provided the

following descriptions: $\bar{\nu}_1$ (symmetric torsional rotation); $\bar{\nu}_2$ (antisymmetric torsional rotation); $\bar{\nu}_3$ (OOO bend); $\bar{\nu}_4$ (symmetric OO stretch); $\bar{\nu}_5$ (antisymmetric OO stretch); $\bar{\nu}_6$ (symmetric HOO bend); $\bar{\nu}_7$ (antisymmetric HOO bend); $\bar{\nu}_8$ (antisymmetric OH stretch); and $\bar{\nu}_9$ (symmetric OH stretch). Within each column of Table II are the frequencies for a particular normal mode as calculated with a variety of basis sets and wave functions. Thus, if the frequencies of two normal modes switch order as the computational level is changed, some rows of the table will not be in strictly increasing order.

Use of the DZP(2d) basis set was not extended to the rather costly MC[14,11] calculations, because comparison of DZP and DZP(2d) frequencies at the RHF and MC[8,8] levels had already shown (Table II) that the extra set of *d* functions had an effects of only about 1%. There was no reason to anticipate a larger basis set effect using the MC[14,11] wave function. The MP2 frequencies were taken from the literature, but the MP4 results were added by us for comparison.

The torsional frequencies $\bar{\nu}_1$ and $\bar{\nu}_2$ decrease by about 15% in going from RHF to MC[8,8] wave functions and then increase by as much as the same amount when the oxygen lone pairs are included in the active space (MC[14,11]). These torsions are expected to be highly very anharmonic, so that their predicted frequencies are not expected to be very accurate. However, the large changes between MC[8,8] and MC[14,11] results indicate that an accurate description of these torsional motions about the O-O bonds should include a correlated description of the oxygen lone pairs.

In the cases of "normal" bending and stretching vibrations, harmonic frequencies calculated at the DZP/RHF level frequently overestimate the observed fundamentals by

10-15%, with the overestimation being reduced to just a few per cent with correlated treatments. This residual overestimation is due to neglect of the anharmonic force constants and basis set limitations, with error cancellations often yielding errors somewhat smaller than might be expected within the harmonic approximation. As shown in Table II, modes 6-9, which involve hydrogen atom motions, follow the usual pattern with the expected decreases in frequency in progressing from RHF to MC[8,8] treatments, and only small changes as the active space is increased to MC[14,11].

The oxygen backbone vibrations, normal modes 3-5, show behavior that departs from the "usual" pattern, with relatively large frequency changes being noted as the computational level is varied. For example, Table II shows that with the DZP basis set, the decreases in frequency from RHF to MC[8,8] are quite large: 19% for $\tilde{\nu}_3$, 29% for $\tilde{\nu}_4$, and 31% for $\tilde{\nu}_5$. In further expanding the treatment of electron correlation the MC[14,11] wave function, the OOO bending motion ($\tilde{\nu}_3$) is unaffected, the symmetric OO stretching frequency ($\tilde{\nu}_4$) increases by about 3%, and the antisymmetric OO stretching frequency ($\tilde{\nu}_5$) further decreases by about 11%. In going from MC[8,8] to MC[14,11] wave functions, the oxygen stretching frequencies not only exhibit rather large changes, *but also switch order*. While both MPBT treatments place the frequencies in the same order as the larger CAS calculations ($\tilde{\nu}_4 > \tilde{\nu}_5$), the changes in going from MP2 to MP4 are unusually large (3-6%) for modes 3-5, again indicating a high sensitivity to the treatment of the correlation energy.

Examination of the MC[14,11] natural orbitals shows that the three nonbonding electron pairs being included in the active space are best described as a 2s-type on the central oxygen atom and a pair of 2p-type on the noncentral oxygens. Attempts to

replace the central oxygen 2s-lone pair with its 2p-lone pair either failed or converged to a higher-energy solution.

3. *Comparison with hydrogen peroxide*

One tool for critical evaluation of the data presented in Table II involves examination of similar computational results for related systems that have well known experimental spectra. In Table III are displayed results of calculations we have carried out for hydrogen peroxide using the same basis sets and comparable MCSCF active spaces. For H_2O_2 the MC[6,6] and MC[10,8] active spaces are analogous, respectively, to the MC[8,8] and MC[14,11] spaces of H_2O_3 . The smaller active space includes only the six bonding electrons in the three sets of nominally bonding and antibonding orbitals, whereas the larger one includes one nonbonding lone pair on each oxygen atom. Table III also shows results for H_2O_2 labelled "MC[14,10]", which include in the active space both lone pairs on each oxygen atom, a calculation which we were not able to carry out on the larger H_2O_3 system. The theoretical H_2O_2 harmonic frequencies and comparable MP2 values³⁹ are reported along with their *ratios* to the *observed* fundamentals.⁴⁰ The MP2 results were chosen for inclusion because they are comparable in both basis set quality and neglect of anharmonicity to the present work; there are much better theoretical values for H_2O_2 available from the same authors and others.^{36,39}

From the ratios in Table III it is seen that the frequencies of the H_2O_2 normal modes that primarily involve hydrogen motion generally follow the usual pattern, with 10-12% decreases in going from RHF to the MC[6,6] level and only a very small change as the active space is further expanded. The frequency changes reported in Table II for $\bar{\nu}_6$ - $\bar{\nu}_9$, the HOO bends and HO stretches in H_2O_3 , follow very much this same pattern. It

is expected that their residual errors will be similar to those for H_2O_2 . The O-O stretch in hydrogen peroxide shown in Table III is overestimated by 33% at the RHF level and underestimated by 5-6% at each of the MCSCF levels. The large change in frequency from RHF to MC[6,6] mirrors closely that of H_2O_3 oxygen-oxygen stretches, $\tilde{\nu}_4$ and $\tilde{\nu}_5$ in Table II. However, the small subsequent change in the H_2O_2 O-O stretch (Table III) in going from MC[6,6] to MC[10,8] is in sharp contrast to the situation for $\tilde{\nu}_4$ and $\tilde{\nu}_5$ of H_2O_3 (Table II) in proceeding from MC[8,8] to MC[14,11]. The large changes and reordering of the OO stretching frequencies of H_2O_3 upon correlation of the oxygen lone pairs do not seem to have precedents in the H_2O_2 results.

4. Comparison with ozone

To further assist in evaluation of the calculated H_2O_3 oxygen backbone vibrational frequencies, it is instructive to consider the vibrational frequencies of ozone, which are well known to be difficult to predict. Lee and Scuseria²⁴ have recently reviewed the literature on this topic. The ground state of ozone has significant biradical character²⁵ and requires a wave function of at least two configurations for a qualitatively correct description. The experimentally derived⁴¹ harmonic vibrational frequencies of ozone are 1135 cm^{-1} (symm. str.), 716 cm^{-1} (bend), and 1089 cm^{-1} (antisymm. str.). At the DZP/SCF level, calculated harmonic vibrational frequencies are found⁴² to be much too large: 36, 18, and 33%, respectively. Improvement of the wave function to the two-configuration level⁴² (TCSCF), which provides a qualitatively correct description of the molecule's biradical character, brings about considerable improvement in the bend and symmetric stretch frequencies (now 9% and 5% too large), but *worse* agreement for the antisymmetric stretch (38% too large), placing the two OO stretches in the wrong order.

Systematic enlargement of the basis set to the TZ2P level does not result in any significant improvement with the TCSCF wave function. Inclusion of external electron correlation *via* either configuration interaction (CISD) based upon both the one- or two-configuration reference states⁴³ or perturbation theory⁴⁴ (MP2 and MP4) based upon a single configuration reference did not result in significant improvement and sometimes yielded results clearly inferior to the uncorrelated ones.

The only approaches to the ozone problem that have yielded significantly improved results are those that include a fairly powerful treatment of the nondynamical electron correlation. A DZP/CASSCF wave function⁴⁵ with the 1s and 2s electrons inactive gave *anharmonic* stretching frequencies that were both too small, but placed in the correct order. The relative errors in comparing the calculated *anharmonic* frequencies with the *observed fundamentals* are: -5% (symm. str.), -2.5% (bend), and -11% (antisymm. str.). In another DZP/CASSCF study⁴⁶ with only the 1s electrons inactive, a trajectory method was used to determine the anharmonic vibrational frequencies for the two stretching motions with the OOO angle fixed at its equilibrium value. When compared to the observed fundamentals, these anharmonic frequencies were found to be in the correct order and in error by only -4% (symm. str.) and -2% (antisymm. str.), a substantial improvement for the antisymmetric stretch. Several coupled-cluster based approaches have been applied to the ozone problem. By incorporating triple excitations *via* the CCSD(T) method and using a large ANO basis set including *f*-functions, Lee and Scuseria²⁴ were able to predict the harmonic frequencies of ozone in the correct order and with errors of less than 3%.

Similarities are apparent between the data in Table II for modes $\bar{\nu}_{3,5}$, the oxygen

backbone vibrations of H_2O_3 , and the O_3 vibrations. Regardless of basis set quality, the frequencies of modes 3-5 of H_2O_3 decrease much more in going from RHF to correlated levels, than the usually expected $\sim 10\%$. As the wave function is improved from the MC[8,8] to MC[14,11] level, which enlarges the active space to include one lone pair on each oxygen atom, the antisymmetric stretching frequency $\bar{\nu}_5$ drops greatly and switches relative order with the symmetric stretch $\bar{\nu}_4$. This is reminiscent of the antisymmetric stretching frequency in ozone, which takes on wildly differing values and also exchanges order with the symmetric stretch as the level of the theoretical treatment is varied. Just as the DZP/CASSCF treatment of ozone yielded frequencies with modest errors that were in the correct order, we expect that the H_2O_3 MC[14,11] results are dependable. In particular, the large changes in $\bar{\nu}_4$ and $\bar{\nu}_5$ between MC[8,8] and MC[14,11] are thought to be significant and not artifacts.

The MP2 and MP4 results which are reported in Table II for comparison, may be somewhat too high, but are probably not greatly in error, as they were in the ozone case. The single reference configuration upon which the MBPT treatment is based is a much better approximation to the H_2O_3 wave function than it is to the essentially biradical ozone ground state. Also presented for comparison are the experimental fundamentals which are available from a study³⁸ of H_2O_3 trapped in a condensate. Because the aqueous condensate would be expected to be hydrogen bonding to the H_2O_3 , we are hesitant to apply these frequencies directly to the predicted gas phase spectrum. However, it is noted that these experimental results are not inconsistent with the expectation that the DZP(+)/MC[14,11] level oxygen-oxygen stretching frequencies may be in error by only a few percent.

5. Absorption intensities

Calculated H₂O₃ infrared absorption intensities are tabulated in Table IV. In going from RHF to correlated calculations, there are considerable changes, particularly for the HO stretches $\tilde{\nu}_8$ and $\tilde{\nu}_9$. Part of this change can be accounted for by a concomitant decrease in the electric dipole moment. The intensity of mode 5, the antisymmetric stretching vibration, undergoes a large decrease in going from RHF to MC[8,8] wave functions, but then experiences even larger increases as the calculation is further enlarged to MC[14,11]. Just as the frequency of this mode is quite sensitive to the treatment of electron correlation, so is its intensity, with the MC[14,11] calculations showing it to be the strongest of the oxygen backbone modes.

The overall picture is of two very intense low frequency torsional vibrations ($\tilde{\nu}_1$ and $\tilde{\nu}_2$), two weak symmetric stretching vibrations ($\tilde{\nu}_4$ and $\tilde{\nu}_9$), and five vibrations of moderate intensity. Augmentation of the basis set from DZP to DZP(2d) does not have a large effect on the pattern of intensities. However, addition of a diffuse function in the DZP(+) basis set is important at the MC(14,11) level, with the intensity of mode 8 (antisymm. OH str.) being doubled and that of mode 3 (-OOO- bend) being reduced by one-third. The MP2 intensities, calculated for comparison, are in reasonable agreement with the MC[14,11] results.

6. Predicted vibrational spectrum

In order to present a theoretical spectrum with the greatest predictive value, we have empirically corrected the calculated frequencies where we can reasonably do so. All of our calculated frequencies are obtained in the harmonic approximation, and this neglect of the anharmonic aspects of the vibrational potential should, by itself, cause the

predicted frequencies to be several percent above the observed fundamentals. However, other shortcomings of the calculation, such as the limited treatment of electron correlation, may cause the harmonic frequencies to be underestimated, with the cancellation of these errors bringing the calculated and observed values into better agreement. We will look to the hydrogen peroxide and ozone examples to obtain estimates of the residual errors in the calculated frequencies.

The estimated absorption intensities are probably less accurate than the frequencies, since they rely on detailed aspects of the charge distribution as well as on the shape of the potential energy surface. As an example, we note the strong variation in intensity in going down the $\tilde{\nu}_8$ column of Table IV even though the corresponding frequency data follow the usual predictable pattern (Table II). General trends in absorption intensities are not as well known, and comparison to experimental numbers is not that straightforward. Consequently, we will base our predicted absorption spectrum on the uncorrected H_2O_3 intensities as calculated at the DZP(+)/MC[14,11] level, our best overall calculation. These intensities should be useful for prediction of overall line strength patterns, but should not be expected to distinguish between lines of similar intensity.

The torsional vibration frequencies of H_2O_3 , $\tilde{\nu}_1$ and $\tilde{\nu}_2$, are left uncorrected beyond the values obtained at the DZP(+)/MC[14,11] level. These vibrations may be expected to have large anharmonic corrections, but will probably not be well characterized by the trends usually found for normal stretches and bends, making a systematic correction impractical. Cremer²² has shown that barriers of only a few kcal mol⁻¹ separate local minima along the path of torsional motion, making it likely that

the spectrum will contain complications arising both from torsional tunnelling and coupling to the other vibrational modes. Detailed treatments such as have been carried out for the torsional mode of H_2O_2 ^{36,39} will probably be needed in order to go much beyond the harmonic estimates given here. The (uncorrected) values used for $\tilde{\nu}_1$ and $\tilde{\nu}_2$ are 337 and 391 cm^{-1} .

The HOO bending and HO stretching frequencies, $\tilde{\nu}_6$ - $\tilde{\nu}_9$, are expected to be well behaved and, therefore, overestimated at the RHF level by about 10-15% and at the CASSCF level by only a few percent. The comparison data in Table III shows that for hydrogen peroxide the overestimation at the MC[10,8] level is 3-4%. Anticipating the same type of behavior for HO stretches and HOO bends in H_2O_3 , we apply a 4% reduction to the DZP(+)/MC[14,11] values in Table II, arriving at the frequencies 1367, 1376, 3566, and 3563 cm^{-1} for $\tilde{\nu}_6$ through $\tilde{\nu}_9$.

While highly accurate harmonic frequencies will generally be higher than the observed fundamentals because of the systematic error due to neglect of anharmonicity, less accurate harmonic frequencies determined at the DZP/CASSCF level may be a few percent above or *below* them. The H_2O_2 data in Table III provides an example where the calculated O-O stretching mode is about 5% below the experimental values. The H_2O_3 oxygen backbone vibrations have already been noted as not fitting the "usual" pattern for well behaved stretches and bends, making uncritical application of the usual corrections somewhat problematic. It has also been observed by us that the behavior of the H_2O_3 modes with improvement of the wave function is similar to that of the ozone vibrations. In particular, the large decrease in frequency from RHF to MCSCF level and the continued large decrease in the antisymmetric stretch frequency as the CASSCF

active space is enlarged are similar to the effects found for ozone. Accordingly, we consider the previous ozone results in order to formulate corrections to modes 3-5.

In the previous ozone work a CASSCF calculation⁴⁵ comparable to the present one yielded anharmonic frequencies that *underestimate* the experimental fundamentals by 3-5% for the bend and symmetric stretch and by about 11% for the antisymmetric stretch. Use of harmonic frequencies in this comparison would have reduced the apparent disagreement by several percent due to cancellation of errors. In fact, the harmonic frequencies cited⁴³ as derived from the work of Ref. 45 differ from the observed fundamentals by: -0.5% (symm str), -2% (bend), -5% (asymm str). Considering both these previously reported errors for ozone and that found by us for the O-O stretch in hydrogen peroxide (Table III), we make the somewhat *ad hoc* assumption that the H₂O₃ DZP(+)/MC[14,11] frequencies of Table II are too low and in error by -2% (symm str and bend) and -5% (asymm. str). Based upon these error estimates, the empirically corrected values of $\tilde{\nu}_{3-5}$ to be used in predicting the spectrum are, respectively, 519, 870, and 760 cm⁻¹. Clearly, this correction procedure is empirical, but we believe it provides estimates of the experimental frequencies that are within 2-3% of the correct gas phase values.

Figures 1 and 2 show a predicted H₂O₃ spectrum in "stick form", with the nine vibrational frequencies $\tilde{\nu}_1$ - $\tilde{\nu}_9$, corrected as described above and the intensities unmodified from the DZP(+)/MC[14,11] results in Table IV. To recognize probable experimental interferences, we also include the observed fundamental frequencies taken from the experimental literature for several other species (HO⁴⁷, HO₂^{48,49,53}, H₂O⁵⁰, and H₂O₂⁴⁰) that are likely to be in the reaction flow tube during the experiment. We obtain

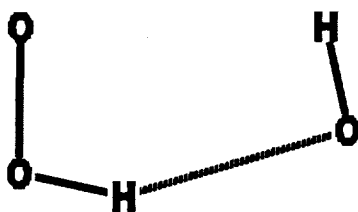
absorption intensities to accompany the experimental frequencies using CASSCF calculations that employ basis sets and active spaces comparable to those used for H_2O_3 . Depending upon the experimental conditions, the concentrations of these interfering species may greatly exceed that of any H_2O_3 formed, so that even intrinsically weak lines could obscure nearby absorptions due to H_2O_3 .

Examination of Figures 1 and 2 shows that the OH stretches and HOO bends of H_2O_3 may well be obscured by other species, depending upon the reaction conditions. However, the vibrations of the H_2O_3 oxygen backbone ($500\text{-}700\text{ cm}^{-1}$) should not suffer significant interference and should be easier to identify. The torsional vibrations are predicted to be very intense. However, their frequencies are probably not well predicted by the present harmonic treatment, and it is not clear how close they might be to the low frequency absorption of hydrogen peroxide.

B. The Hydrogen-Bonded HO...HOO Species.

1. *Equilibrium geometry*

In previous studies,^{15,20,21} the ground state of the hydrogen bonded complex was



HO ... HOO Hydrogen-bonded Intermediate

found to be planar and display $^3A'$ symmetry, with the unpaired electrons on each radical situated in out-of-plane a'' orbitals. The predictions made by these authors of the stability of the complex relative to the separated radicals fell in the range 4.5 - 9.0 kcal mol⁻¹. The $^3A'$ state is treated here even though it does not correlate through planar conformations with the ground state products of reaction (1). We are focusing on intermediate species that might be stabilized and detected, regardless of whether or not they are likely to proceed to products. The MC[10,9] calculations reported for HO \cdots HOO in Tables V-VI have active spaces that include ten electrons in three a' (σ -type) bonding orbitals, three a' (σ^* -type) antibonding orbitals, and three a'' out-of-plane (π and π^* of HO $_2$; $2p$ of HO \cdot) orbitals. None of the in-plane a' lone pairs on the oxygens are included in the active space.

The minimum energy conformation of the HO \cdots HOO complex found at the various levels of theory in the present study is consistent with the previous work. As shown in Table V, the intramolecular coordinates are found to be only slightly perturbed from those of the uncomplexed radicals. This is even true for the R_{OO} coordinate of HO $_2$, which is highly sensitive to the treatment of electron correlation. The MP2 and MCSCF results differ by ~ 0.04 Å and bracket the experimental value⁵¹ of 1.331 Å. Even though the various R_{OO} values in Table V differ by as much as 0.05 Å, the changes in R_{OO} upon complexation fall in the range 0.002-0.008 Å for each of the methods tabulated.

As anticipated because the potential well of the complex is quite shallow, its intermolecular coordinates display greater sensitivity both to the basis set used and to the treatment of electron correlation. These parameters would probably undergo

considerable change as further improvements in the basis set and electron correlation treatment are made. One interesting difference between the results obtained by the different methods is that the $R_{O\cdots H}$ distance *increases* in going from the ROHF to the CASSCF treatment, whereas it *decreases* in going from ROHF to MP2. While the present study has not considered the $^3A''$ state of the complex, previous studies^{15,20} have shown that these intermolecular parameters may be considerably different for that electronic state, in which the unpaired electron of the hydroxyl radical is rotated into the plane of the complex.

2. *Vibrational frequencies*

In table VI are given the harmonic vibrational frequencies as calculated for the hydrogen bonded $HO\cdots HOO$ species. The intermolecular vibrational modes $\tilde{\nu}_1$ - $\tilde{\nu}_5$, which appear in the spectrum only upon complex formation, are probably not well described within the harmonic approximation, and their frequencies may not be accurately predicted. While all of the intermolecular mode frequencies increase as electron correlation is included in the calculation, modes 2 and 5 show unusually large increases. If these calculated results are accurate and modes 2 and 5 appear in the range of 700-800 cm^{-1} , as indicated by the MC[10,9] calculations, they would be at higher frequency than the OOO bend and near the antisymmetric O-O stretch in the covalent HOOOH species.

Normal modes 2 and 5 are shown, respectively, in Figures 3 and 4 at both the ROHF and MC[10,9] levels. These modes are seen to involve mostly out of plane motions of the hydrogen atoms. At the ROHF level, mode 2 is mainly a rocking motion of the hydroxyl radical (Fig. 3) and mode 5 (Fig. 4) is primarily a rocking motion of the

hydroperoxyl radical. At the MCSCF level, these modes show coupled motions of the two radicals. Mode 2, while still primarily a rocking motion of the OH radical, includes an out-of-phase rock of the HO₂· species. In the same way mode 5 changes from almost pure HO₂· motion to an in-phase rocking of both radicals. Because use of a correlated wave function had such a large effect on the frequencies of modes 2 and 5, the DZP/MP2 method was also employed to provide a comparison. While the effect is not as large as with the CASSCF approach, modes 2 and 5 still undergo substantial increases and mode 4, an in-plane motion, shows an unusually large change.

It is not clear from examination of the wave functions, charge distributions, and force constants why these α'' out-of-plane modes are affected so much by inclusion of electron correlation. Two of the three leading configurations after the SCF reference one, however, involve the $\pi \rightarrow \pi^*$ excitation on HO₂·, either by itself as a single excitation or as part of the $\sigma\pi \rightarrow \sigma^*\pi^*$ double excitation. Since the π orbital is localized mostly on the central oxygen, and the π^* orbital mostly on the terminal oxygen, these important excitations move a significant amount of negative charge to the terminal oxygen of HO₂·. This increased charge would be expected to enhance the electrostatic attraction between the hydroperoxyl terminal oxygen and the hydrogen end of the hydroxyl radical, resulting in a larger force constant for out-of-plane motion of that hydrogen atom. In fact the out-of-plane force constant for the hydroxyl hydrogen increases by about 30-fold, from 0.0006 to 0.018 hartree bohr⁻¹ in going from ROHF to MC[10,9] wave function. However, this explanation is at best incomplete, as there is not a similar increase in charge at the hydroxyl oxygen to account for the 4-fold enhancement of the out-of-plane force constant for the hydroperoxyl hydrogen atom with

inclusion of electron correlation.

The HO...HOO intramolecular modes have descriptions and frequencies very much the same as those of the isolated radicals. In the spectra of weakly interacting systems, it is often the *shifts* of these similar vibrational frequencies upon complex formation that are most easily characterized. Experience in this laboratory⁵² in comparing calculated and experimental frequency shifts for the water dimer, has indicated that, although the absolute frequencies are much improved upon inclusion of electron correlation, the *frequency shifts* are more accurately calculated at the SCF level than at MCSCF levels comparable to those used in this work. It was found in that study that CASSCF results frequently underestimated the shifts by large amounts, sometimes assigning them the wrong sign. The MP2 results in that study tended to very badly overestimate the frequency shifts, with only the shifts calculated at the SCF level having consistently correct signs and reasonable magnitudes. Further, these SCF level frequency shifts were not very sensitive to augmentation of the basis set beyond the DZP level.

In Table VII are tabulated the differences between the harmonic vibrational frequencies in the HO...HOO complex and in the isolated radicals, as determined in parallel calculations. Following our experience⁵² with the water dimer, we expect that the ROHF/DZP(+,2d) shifts are the most accurate predictions in Table VII. The frequencies with large shifts, particularly the HO stretch and HOO bend in HO₂, are likely to have the greatest diagnostic value.

The large difference between the CASSCF and MP2 values for $\bar{\nu}_6$ (the O-O stretch) reported for the complex in Table VI is similar to the difference found between the same methods for isolated HO₂. In that case, the experimental fundamental⁵³ of

the O-O stretch is 1098 cm^{-1} and the CASSCF value (1048 cm^{-1}) is in much better agreement. Presumably, the CASSCF value for $\bar{\nu}_6$ in the complex is also closer to the experimental one.

3. Absorption intensities

In Table VIII are shown the calculated absorption intensities for the hydrogen bonded complex of H_2O_3 . All of the intermolecular vibrations of the complex, modes 1-5, have significant intensities, with the two out-of-plane (a") vibrations (modes 2 and 5) and the in-plane rotation of the hydroxyl radical (mode 4) being particularly strong. Of the intramolecular vibrational modes, the intensities of modes 6-7, the O-O stretch and HOO bend in HO_2 , do not change much upon complexation. However, the HO stretch of HO_2 (mode 8) is predicted at all levels of theory to become 3-4 times more intense in the complex than in the isolated radical. The hydroxyl radical HO stretch (mode 9) is also predicted by all of the calculations to grow in intensity upon complex formation. The experimental intensity of the $\text{HO}\cdot$ vibration is weak, and the MCSCF results for the isolated radical are probably more accurate than are the ROHF results, suggesting a 15-fold increase in intensity upon complex formation.

The decrease in intensity for mode 2 in going from ROHF to MC[10,9] results can be understood from the normal mode sketch in Fig. 3. At the MCSCF level the coupling of the two hydrogen rocking motions causes the two OH bond dipoles to move out of the plane in opposite directions, reducing the overall change in dipole moment and causing the intensity to drop from 128 to 42 km/mol. In the case of mode 5, the coupling of the rocking motions causes both bond dipoles to move out of plane in the same direction, increasing the overall change in dipole moment and causing a small

intensity increase from ROHF to MC[10,9].

IV. CONCLUSIONS

Theoretical values for the infrared absorption spectrum of both the covalent and hydrogen bonded isomers of the complex formed between the hydroxyl and hydroperoxyl radicals have been presented. For the covalent HOOOH species, the vibrational frequencies of the stiff modes (bends and stretches) have been predicted with an expected accuracy of a few percent. Consideration of the spectra of possible interferents (Figs. 1 and 2), suggests that the relatively strong absorptions due to the bending motions and antisymmetric stretch of the O-O-O backbone may be the most easily identified and characterized. These are predicted to occur at 518 and 756 cm^{-1} . The stronger absorptions due to the torsional motions of HOOOH may also be useful for this purpose, but it is expected that these vibrations are not as well treated within the harmonic approximation and may be less accurately predicted.

Formation of the hydrogen bonded $\text{HO}\cdots\text{HO}_2$ complex gives rise to five new interradical modes of vibration. Some of these are predicted to be quite intense and may be useful for detection of the species. Noteworthy in this regard are the out-of-plane motions of the hydrogen atoms, denoted $\bar{\nu}_2$ and $\bar{\nu}_5$, which at the best computational level are predicted to lie in the region 700-800 cm^{-1} . However, these frequencies show a very strong dependence on the theoretical level and are probably not well treated in the harmonic approximation, indicating that their predicted values should not be considered highly accurate. These uncertainties considerably lessen the utility of these modes for identification purposes. The frequency shifts of the internal vibrational modes, especially the HO stretch and HOO bend in the HO_2 radical, are probably more accurately predicted and should be most useful for detection of the $\text{HO}\cdots\text{HOO}$ species.

The large intensity increase predicted for the hydroxyl radical stretching vibration upon complexation may also make that mode useful.

In addition to predicting features of the absorption spectra of these two species, we note two other interesting features of this study. In the case of the covalent HOOOH species, the magnitude and relative order of the O-O-O backbone symmetric and antisymmetric stretching mode frequencies are very sensitive to the level of theoretical treatment. This is quite similar to the situation previously found for the ozone molecule. In that case, the interpretation was complicated by the difficulty in separating effects due to the biradical character of ozone's electronic ground state from other aspects of the electron correlation problem. In the present case, however, the closed shell singlet reference state is a good zeroth order wave function and similar difficulties still arise here. Because enlarging the active space to include the oxygen atom lone pairs has so much larger effect on $\tilde{\nu}_5$ (antisymmetric stretch) than on $\tilde{\nu}_4$ (symmetric stretch), it seems clear that this additional correlation becomes increasingly important as the molecule is distorted away from C_2 symmetry. An attempt was made to identify specific configurations that increased in importance in the CAS wave function as the molecular framework was distorted small amounts along the antisymmetric -OOO- stretch. However, examination of these C_1 and C_2 wave functions did not reveal any important changes among the configurations with $|c_i| \geq 0.025$. Recalling that inclusion of both lone pairs on each oxygen atom, rather than just one, provided further improvement in the ozone case⁴⁶, we anticipate that $\tilde{\nu}_5$ in the present study would also be improved by further expansion of the active space. However, we are not able to carry out that larger study at this time.

In the case of the hydrogen bonded species, certain of the intermolecular vibrations have predicted frequencies that are very sensitive to the inclusion of electron correlation *via* CASSCF, with $\tilde{\nu}_2$ and $\tilde{\nu}_5$ increasing relative to the ROHF results by factors of 2-3. These out-of-plane modes, which mostly involve hydrogen atom motions, move from quite low frequencies (100-400 cm^{-1}) at the RHF level into the 700-800 cm^{-1} region at the MC[10,0] level.

V. ACKNOWLEDGEMENTS

Funding and computational resources for this work were provided by the National Aeronautics and Space Administration (NCC1-55), the National Science Foundation Chemical Instrumentation Program (CHE-8913800), and the North Carolina Supercomputing Center. Helpful discussions with Donald H. Phillips and Geoffrey E. Quelch are also gratefully acknowledged.

VI. REFERENCES

1. a) W. Hack, A.W. Preuss, and H. Gg. Wagner, *Ber. Bunsenges. Phys. Chem.* **82**, 1167 (1978)
b) F. Temps and H. Gg. Wagner, *Ber. Bunsenges. Phys. Chem.* **86**, 119 (1982)
2. a) J.S. Chang and F. Kaufman, *J. Phys. Chem.* **82**, 1683 (1978)
b) U.C. Sridharan, L.X. Qiu and F. Kaufman, *J. Phys. Chem.* **85**, 3361 (1981)
3. J.P. Burrows, D.I. Cliff, G.W. Harris, B.A. Thrush, and J.P.T. Wilkinson, *Proc. R. Soc. Lond. A* **368**, 463 (1979)
4. L.F. Keyser, *J. Phys. Chem.* **85**, 3667 (1981)
5. a) W.B. DeMore and E. Tschuikow-Roux, *J. Phys. Chem.* **78**, 1447 (1974)
b) W.B. DeMore, *J. Phys. Chem.* **86**, 121 (1982)
6. C.J. Hochanadel, T.J. Sworski, and P.J. Ogren, *J. Phys. Chem.* **84**, 3274 (1980)
7. M.J. Kurylo, O. Klais and A.H. Laufer, *J. Phys. Chem.* **85**, 3674 (1981)
8. R.A. Cox, J.P. Burrows and T.J. Wallington, *Chem. Phys. Lett.* **84**, 217 (1981)
9. R-R. Lii, R.A. Gorse, Jr., M.C. Sauer, Jr. and S. Gordon, *J. Phys. Chem.* **84**, 819 (1980)
10. M. Braun, A. Hofzumahaus and F. Stuhl, *Ber. Bunsenges. Phys. Chem.* **86**, 597 (1982)
11. U.C. Sridharan, L.X. Qiu and F. Kaufman, *J. Phys. Chem.* **88**, 1281 (1984)
12. V.B. Rozenshtein, Y.M. Gershenzon, S.D. Il'in and O.P. Kishkovitch, *Chem. Phys. Lett.* **112**, 473 (1984)
13. P. Dransfeld and H. Gg. Wagner, *Z. Naturforsch.* **42a**, 471 (1987)
14. M. Mozurkewich, *J. Phys. Chem.* **90**, 2216 (1986)
15. D.W. Toohey and J.G. Anderson, *J. Phys. Chem.* **93**, 1049 (1989)

16. L.F. Keyser, *J. Phys. Chem.* **92**, 1193 (1988)
17. J.J. Schwab, W.H. Brune and J.G. Anderson, *J. Phys. Chem.* **93**, 1030 (1989)
18. NASA, *Chemical Kinetics and Photochemical Data for Use in Stratospheric Modeling*, Evaluation No. 9, NASA Panel for Data Evaluation, Publication 90-1 (Jet Propulsion Laboratory, Pasadena, 1990)
19. C. Gonzalez, J. Theisen, H.B. Schlegel, W.L. Hase and E.W. Kaiser, *J. Phys. Chem.* **95**, 6784 (1991)
20. C. Gonzalez, J. Theisen, H.B. Schlegel, W.L. Hase and E.W. Kaiser, *J. Phys. Chem.* **96**, 1767 (1992)
21. C.F. Jackels and D.H. Phillips, *J. Chem. Phys.* **84**, 5013 (1986). See references therein for earlier computational studies.
22. D. Cremer, *J. Chem. Phys.* **69**, 4456 (1978)
23. J.P.D. Abatt, K.L. Demerjian, and J.G. Anderson, *J. Phys. Chem.* **94**, 4566 (1990)
24. T.J. Lee and G.E. Scuseria, *J. Chem. Phys.* **93**, 489 (1990), and references cited therein.
25. W.A. Goddard III, T.H. Dunning Jr., W.J. Hunt and P.J. Hay, *Acc. Chem. Res.* **6**, 368 (1973)
26. T.H. Dunning, Jr., *J. Chem. Phys.* **53**, 2823 (1970).
27. S. Huzinaga, *J. Chem. Phys.* **42**, 1293 (1965).
28. a) W.J. Hehre, R. Ditchfield and J.A. Pople, *J. Chem. Phys.* **56**, 2257 (1972);
b) P.C. Hariharan and J.A. Pople, *Theor. Chim. Acta* **28**, 213 (1973).
29. a) B.O. Roos, P.R. Taylor and P.E.M. Siegbahn, *Chem. Phys.* **48**, 157 (1980); b) for a review of the CASSCF method see B. O. Roos in *Ab initio Methods in Quantum*

- Chemistry, Part II*, edited by K.P. Lawley, *Advances in Chemical Physics, Vol LXIX* (John Wiley & Sons, Chichester, 1987), pp. 399-446.
30. M. Dupuis, P. Mougnot, J.D. Watts, G.J.B. Hurst and H.O. Villar in *Modern Techniques in Computational Chemistry: MOTECC-89*, edited by E. Clementi, (ESCOM Science Publishers, Leiden, 1989), Ch. 7. The MCSCF algorithms used in the GAMESS package are taken largely from HONDO7, which is described in this reference.
 31. J. Baker, *J. Comput. Chem.* **7**, 385 (1986)
 32. J.S. Binkley and J.A. Pople, *Int. J. Quantum Chem.* **9**, 229 (1975); J.A. Pople, J.S. Binkley and R. Seeger, *ibid.* **S10**, 1 (1976); R. Krishnan and J.A. Pople, *ibid.* **14**, 91 (1978).
 33. G. Zerbi in *Vibrational Intensities in Infrared and Raman Spectroscopy*, edited by W. B. Person and G. Zerbi, (Elsevier Scientific, Amsterdam, 1982), Chap. 3, pp. 23-66.
 34. M.W. Schmidt, K.K. Baldrige, J.A. Boatz, J.H. Jensen, S. Koseki, M.S. Gordon, K.A. Nguyen, T.L. Windus and S.T. Elbert, *Quantum Chemistry Program Exchange Bulletin* **10**, 52 (1990); M. Dupuis, D. Spangler and J.J. Wendoloski, *National Resource for Computations in Chemistry Software Catalog*, (University of California, Berkeley, California, 1980), Program QG01.
 35. M.J. Frisch, M. Head-Gordon, G.W. Trucks, J.B. Foresman, H.B. Schlegel, K. Raghavachari, M.A. Robb, J.S. Binkley, C. Gonzalez, D.J. Defrees, D.J. Fox, R.A. Whiteside, R. Seeger, C.F. Melius, R. Baker, R.L. Martin, L.R. Kahn, J.J.P. Stewart, S. Topiol and J.A. Pople, Gaussian, Inc., Pittsburgh, Pennsylvania, 1990.
 36. L.B. Harding, *J. Phys. Chem.* **93**, 8004 (1989)

37. J. Koput, *J. Mol. Spectrosc.* **115**, 438 (1986)
38. J.L. Arnau and P.A. Giguere, *J. Chem. Phys.* **60**, 270 (1974); P.A. Giguere, *Trans. N.Y. Ac. Sc. Series II* **34**, 334 (1972).
39. A. Willetts, J.F. Gaw and N.C. Handy, *J. Mol. Spectrosc.* **135**, 370 (1989)
40. G.A. Khachkuruzov and I.N. Przhevalskii, *Opt. Spectrosc.* **41**, 323 (1976)
41. A. Barbe, C. Secroun and P. Jouve, *J. Mol. Spectrosc.* **49**, 171 (1974)
42. Y. Yamaguchi, M.J. Frisch, T.J. Lee, H.F. Schaefer III and J. S. Binkley, *Theor. Chim. Acta* **69**, 337 (1986)
43. T.J. Lee, W.D. Allen and H.F. Schaefer III, *J. Chem. Phys.* **87**, 7062 (1987)
44. G.E. Scuseria, T.J. Lee, A.C. Scheiner and H.F. Schaefer III, *J. Chem. Phys.* **90**, 5635 (1989)
45. S.M. Adler-Golden, S.R. Langhoff, C.W. Bauschlicher, Jr., and G.D. Carney, *J. Chem. Phys.* **83**, 255 (1985)
46. M.L. Koszykowski and C. M. Rohlfing, *Chem. Phys. Lett.* **142**, 67 (1987)
47. G. Herzberg, *Molecular Spectra and Molecular Structure, Volume I*, (Van Nostrand Reinhold Co, New York, 1950), Table 39, p. 560; calculated as $\omega_e - 2\omega_e x_e$.
48. C. Yamada, Y. Endo and E. Hirota, *J. Chem. Phys.* **78**, 4379 (1983)
49. K. Nagai, Y. Endo, and E. Hirota, *J. Mol. Spectrosc.* **89**, 520 (1981)
50. G. Herzberg, *Molecular Spectra and Molecular Structure, Vol III*, (Van Nostrand Reinhold, New York, 1966), Table 62, p. 585.
51. H. Uehara, K. Kawaguchi and E. Hirota, *J. Chem. Phys.* **83**, 5479 (1985)
52. D.M. Haskins and C.F. Jackels, "Calculated Vibrational Frequency Shifts of the Water Dimer", presented at the Fifth National Conference on Undergraduate Research, Pasadena, California, March, 1991.

53. J.W.C. Johns, A.R.W. McKellar and M. Rigglin, *J. Chem. Phys.* **68**, 3957 (1978)

TABLE I. Minimum Energy Conformation of 1A HOOH.^a

METHOD	R_{OH}	R_{OO}	θ_{OOO}	θ_{HOO}	ϕ_{HOOO}
DZP Basis					
RHF	0.950	1.369	107.5	103.8	81.4
MC[8,8]	0.975	1.460	105.1	100.0	81.2
MC[14,11]	0.976	1.457	106.7	100.1	80.7
DZP(+) Basis					
RHF	0.950	1.368	107.6	103.9	81.8
MC[8,8]	0.975	1.458	105.2	100.2	81.5
MC[14,11]	0.976	1.456	106.8	100.4	81.4
DZP(2d) Basis					
RHF	0.948	1.368	107.6	103.7	80.5
MC[8,8]	0.973	1.458	105.1	100.0	79.0
MC[14,11]	0.974	1.456	106.7	100.2	79.8
6-31G [*] /MP2 ^b	0.972	1.439	106.3	100.2	78.1

- a. Units are Angstroms and degrees. The molecule has C_2 symmetry. R_{AB} is the AB bond distance; θ_{ABC} is the included angle formed by the AB and BC bonds; ϕ_{HOOO} is the dihedral angle formed by the OOO and HOO planes.
- b. Reference 22 ; see also Reference 19 for similar results obtained with the slightly larger 6-31G^{**} basis set.

TABLE II. Vibrational Frequencies (in cm^{-1}) for Covalent H_2O_3^a .

METHOD	Normal Mode								
	$\bar{\nu}_1$	$\bar{\nu}_2$	$\bar{\nu}_3$	$\bar{\nu}_4$	$\bar{\nu}_5$	$\bar{\nu}_6$	$\bar{\nu}_7$	$\bar{\nu}_8$	$\bar{\nu}_9$
DZP Basis									
RHF	397	426	627	1142	1182	1565	1572	4128	4132
MC[8,8]	335	363	509	808	816	1404	1422	3739	3741
MC[14,11]	368	425	509	833	725	1391	1403	3720	3722
DZP(+) Basis									
RHF	385	414	629	1143	1181	1562	1572	4123	4126
MC[8,8]	323	348	508	808	818	1403	1418	3736	3738
MC[14,11]	337	391	509	853	724	1424	1433	3715	3711
DZP(2d) Basis									
RHF	394	433	629	1125	1159	1578	1586	4125	4128
MC[8,8]	336	366	511	801	814	1419	1429	3737	3739
6-31G** Basis									
MP2 ^b	366	417	537	904	829	1395	1399	3792	3796
MP4(SDTQ)	364	417	520	868	783	1383	1387	3781	3785
Exptl ^c			500	855	755				

- a. Theoretical frequencies are harmonic. Experimental frequencies are observed fundamentals in condensate. See text for qualitative description of normal modes.
- b. Reference 19
- c. Reference 38

TABLE III. Calculated Harmonic Vibrational Frequencies for Hydrogen Peroxide (in cm^{-1}). Ratios to Observed Fundamentals^a are Shown in Parentheses. DZP Basis Set used Throughout.

METHOD	Normal Mode Description				
	OO str	$\theta_{\text{HOO,symm}}$	$\theta_{\text{HOO,asym}}$	HO str _{symm}	HO str _{asym}
RHF	1168 (1.33)	1604 (1.16)	1474 (1.16)	4169 (1.16)	4169 (1.15)
MC[6,6]	826 (0.94)	1445 (1.04)	1317 (1.04)	3763 (1.05)	3766 (1.04)
MC[10,8]	833 (0.95)	1438 (1.04)	1309 (1.03)	3741 (1.04)	3746 (1.04)
MC[14,10]	824 (0.94)	1411 (1.02)	1284 (1.01)	3737 (1.04)	3741 (1.04)
MP2 ^b	932 (1.07)	1435 (1.03)	1308 (1.03)	3864 (1.07)	3863 (1.07)

a. Experimental Fundamentals used in determining ratios: 875, 1387, 1266, 3599, and 3611 cm^{-1} , respectively. See Reference 40.

b. Reference 39.

TABLE IV. Absorption Intensities (in km/mol)^a for Covalent H₂O₃^b.

METHOD	Normal Mode								
	$\bar{\nu}_1$	$\bar{\nu}_2$	$\bar{\nu}_3$	$\bar{\nu}_4$	$\bar{\nu}_5$	$\bar{\nu}_6$	$\bar{\nu}_7$	$\bar{\nu}_8$	$\bar{\nu}_9$
DZP Basis									
RHF	172.0	132.2	36.6	3.2	37.4	34.6	56.2	121.3	9.0
MC[8,8]	137.8	114.5	29.6	7.2	15.6	37.6	63.4	36.8	2.5
MC[14,11]	123.0	114.9	44.8	7.2	58.3	35.9	57.9	34.6	2.5
DZP(+) Basis									
RHF	176.2	133.5	34.2	2.7	39.3	34.6	51.1	134.8	8.9
MC[8,8]	142.0	115.4	24.9	5.9	17.3	38.0	58.3	43.1	3.0
MC[14,11]	126.3	110.3	31.3	6.8	61.7	43.1	63.0	72.7	10.1
DZP(2d) Basis									
RHF	153.8	122.1	29.6	2.9	34.2	36.3	60.0	125.5	9.7
MC[8,8]	120.4	109.4	24.1	6.3	14.8	39.7	65.5	43.9	3.6
6-31G**									
MP2	125.7	134.4	40.2	9.0	59.7	36.5	63.0	53.4	4.3

a. 1 km/mol = 42.255 D²/amu·Å².

b. See text for qualitative description of normal modes.

TABLE V. Minimum Energy Conformation of $^3A'$ Hydrogen-Bonded $\text{HO}\cdots\text{HO}\cdots\text{HO}$ Complex^a. Conformations of Isolated HO and HO_2 Species Shown in Italics.

METHOD	HO ₂ Coordinates		OH Coordinate R_{OH}	Intermolecular Coordinates		
	R_{OH}	R_{OO} Θ_{HO}		$R_{\text{O}\cdots\text{H}}$	$\Theta_{\text{HO}\cdots\text{H}}$	$\Theta_{\text{OH}\cdots\text{O}}$
<u>ROHF</u> DZP	0.954	1.310 105.22	0.957	2.078	104.70	152.03
	<i>0.950</i>	<i>1.312 105.89</i>	<i>0.956</i>			
DZP(+)	0.954	1.309 105.44	0.957	2.082	112.1	157.72
	<i>0.951</i>	<i>1.311 105.99</i>	<i>0.956</i>			
DZP(+,2d)	0.952	1.305 105.37	0.955	2.091	102.87	154.13
	<i>0.949</i>	<i>1.307 105.90</i>	<i>0.954</i>			
<u>MC[10,9]</u> DZP(+,2d)	0.978	1.355 102.45	0.978	2.129	95.00	150.31
	<i>0.975</i>	<i>1.358 102.76</i>	<i>0.977</i>			
<u>MP2^b</u> 6-31G ^{**}	0.984	1.317 103.5	0.978	1.943	80.5	140.6
	<i>0.975</i>	<i>1.325 104.5</i>	<i>0.971</i>			

a. Planar molecule; bond lengths in Angstroms; bond angles in degrees.

b. Reference 20

TABLE VI. Harmonic Vibrational Frequencies (in cm^{-1}) for $^3A'$ Hydrogen-bonded HO...HOO Complex. Results for Uncomplexed Species Shown in Italics.

METHOD	$\tilde{\nu}_1$	$\tilde{\nu}_2$	$\tilde{\nu}_3$	Normal Mode ^a					
				$\tilde{\nu}_4$	$\tilde{\nu}_5$	$\tilde{\nu}_6$	$\tilde{\nu}_7$	$\tilde{\nu}_8$	$\tilde{\nu}_9$
<u>ROHF</u>									
DZP	61	148	178	333	403	1274	1652	4051	4072
						<i>1270</i>	<i>1594</i>	<i>4104</i>	<i>4082</i>
DZP(+)	56	121	169	314	383	1276	1650	4053	4077
						<i>1272</i>	<i>1596</i>	<i>4102</i>	<i>4085</i>
DZP(+,2d)	60	134	165	339	387	1247	1664	4036	4063
						<i>1242</i>	<i>1611</i>	<i>4095</i>	<i>4079</i>
<u>MC[10,9]^b</u>									
DZP(+,2d)	104	723	176	363	772	1065	1532	3670	3686
						<i>1048</i>	<i>1474</i>	<i>3692</i>	<i>3680</i>
<u>MP2</u>									
DZP(+,2d)	138	268	215	487	467	1262	1533	3527	3752
						<i>1208</i>	<i>1454</i>	<i>3708</i>	<i>3828</i>

- a. Normal mode identifications: $\tilde{\nu}_{1,3,4}$ (intermolecular in-plane (a') modes); $\tilde{\nu}_{2,5}$ (intermolecular out-of-plane (a'') modes); $\tilde{\nu}_6$ (O-O stretch); $\tilde{\nu}_7$ (HOO bend); $\tilde{\nu}_8$ (HO stretch in HO₂); and $\tilde{\nu}_9$ (HO stretch in HO). These labels are used for similar modes in the isolated species.
- b. MC[10,9] for complex, MC[7,6] for HO₂, and MC[3,3] for HO.

TABLE VII. Calculated Frequency Shifts (in cm^{-1}) for $^3\text{A}'$ $\text{HO}\cdots\text{HOO}$ upon Complexation.^a

METHOD	HO_2 Modes($\tilde{\nu}_6$ - $\tilde{\nu}_8$)			OH Mode($\tilde{\nu}_9$)
	OO Str	HOO Bend	HO Str	OH Str
<u>ROHF</u>				
DZP Basis	4	58	-53	-10
DZP(+)	4	54	-49	-7
DZP(+,2d)	5	53	-59	-16
<u>MCSCF^b</u>				
DZP(+,2d)	17	58	-22	6
<u>MP2</u>				
DZP(+,2d)	54	79	-181	-76

a. Calculated as: $\tilde{\nu}_i(\text{complex}) - \tilde{\nu}_i(\text{uncomplexed radical})$

b. MC[10,9] for complex, MC[7,6] for HO_2 , and MC[3,3] for HO.

TABLE VIII. Absorption Intensities for Hydrogen-bonded HO...HOO (in km/mol)^a Results for Uncomplexed Species Shown in Italics.

METHOD	Normal Mode ^a								
	$\tilde{\nu}_1$	$\tilde{\nu}_2$	$\tilde{\nu}_3$	$\tilde{\nu}_4$	$\tilde{\nu}_5$	$\tilde{\nu}_6$	$\tilde{\nu}_7$	$\tilde{\nu}_8$	$\tilde{\nu}_9$
<u>ROHF</u>									
DZP	44.4	136.5	25.8	147.0	221.8	37.2 <i>40.1</i>	63.0 <i>56.2</i>	215.1 <i>58.7</i>	60.4 <i>23.7</i>
DZP(+)	31.7	147.0	20.7	147.0	210.9	38.9 <i>41.0</i>	54.1 <i>51.6</i>	251.4 <i>67.6</i>	58.7 <i>30.4</i>
DZP(+,2d)	36.3	128.5	24.5	143.2	186.3	36.8 <i>39.3</i>	56.6 <i>55.4</i>	241.7 <i>70.6</i>	66.8 <i>34.2</i>
<u>MC[10,9]^b</u>									
DZP(+,2d)	24.9	41.8	48.2	125.1	211.3	23.7 <i>28.3</i>	72.7 <i>71.0</i>	141.6 <i>39.3</i>	46.1 <i>3.5</i>
<u>MP2</u>									
DZP(+,2d)	68.9	130.2	52.3	162.5	160.9	88.7 <i>98.7</i>	50.7 <i>33.1</i>	305.1 <i>55.6</i>	67.5 <i>22.4</i>

- a. Normal mode identifications: $\tilde{\nu}_{1,3,4}$ (intermolecular in-plane (a') modes); $\tilde{\nu}_{2,5}$ (intermolecular out-of-plane (a'') modes); $\tilde{\nu}_6$ (O-O stretch); $\tilde{\nu}_7$ (HOO bend); $\tilde{\nu}_8$ (HO stretch in HO₂); and $\tilde{\nu}_9$ (HO stretch in HO). These labels are used for similar modes in the isolated species.
- b. MC[10,9] for complex, MC[7,6] for HO₂, and MC[3,3] for HO.

LIST OF FIGURES

- Figure 1. Predicted Spectrum (200 - 1800 cm^{-1}) of Covalent HOOOH with Possible Interfering Species. Experimental Frequencies: HO_2 , H_2O_2 , and H_2O .
- Figure 2. Predicted Spectrum (3200 - 3800 cm^{-1}) of Covalent HOOOH with Possible Interfering Species. Experimental Frequencies: HO , HO_2 , H_2O_2 , and H_2O .
- Figure 3. Normal Mode No. 2 for $^3\text{A}'$ $\text{HO}\cdots\text{HOO}$: a) ROHF ($\tilde{\nu}_2 = 134 \text{ cm}^{-1}$); b) MC[10,9] ($\tilde{\nu}_2 = 723 \text{ cm}^{-1}$).
- Figure 4. Normal Mode No. 5 for $^3\text{A}'$ $\text{HO}\cdots\text{HOO}$: a) ROHF ($\tilde{\nu}_5 = 387 \text{ cm}^{-1}$); b) MC[10,9] ($\tilde{\nu}_5 = 772 \text{ cm}^{-1}$).

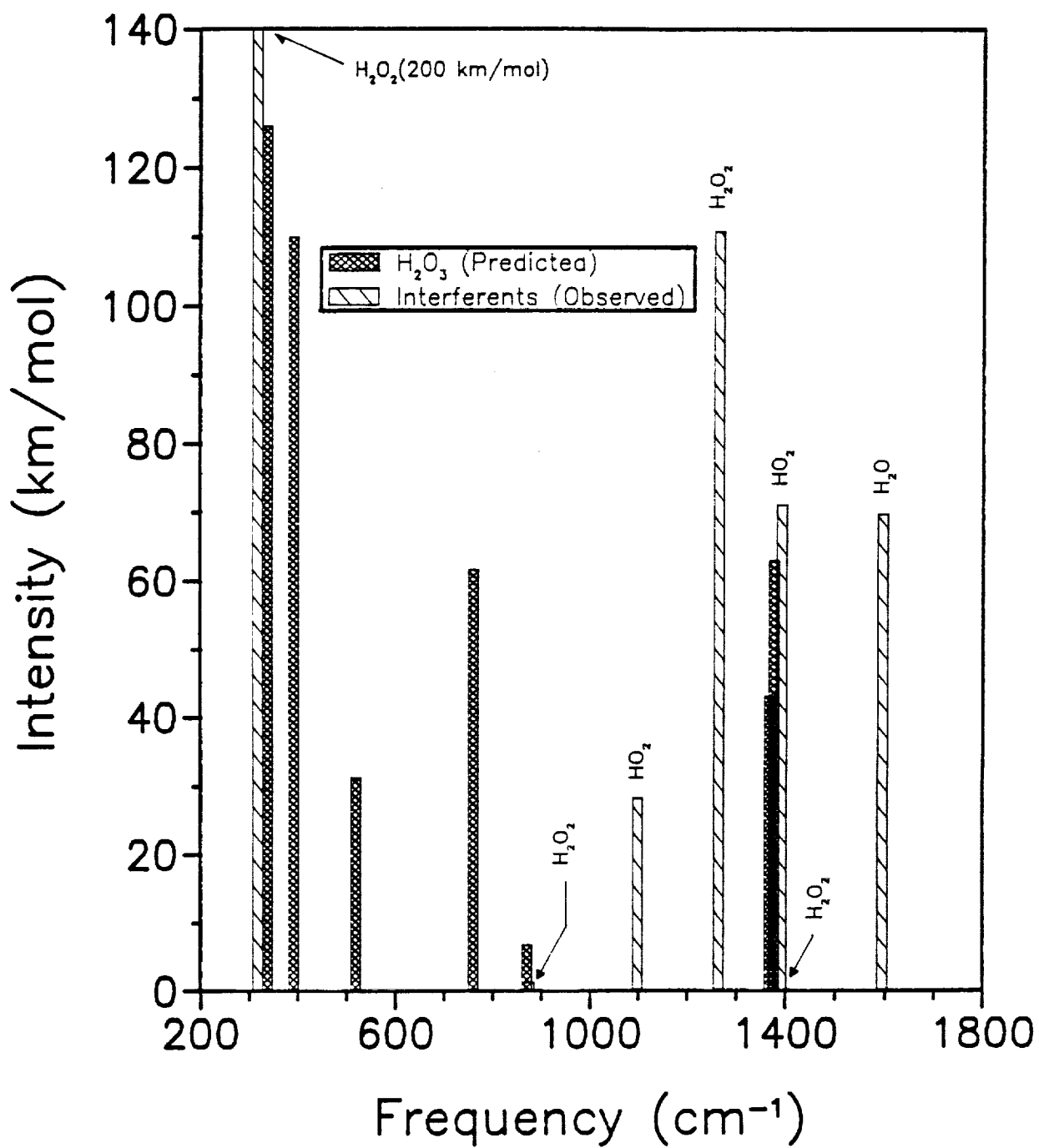


Figure 1 - Jackels

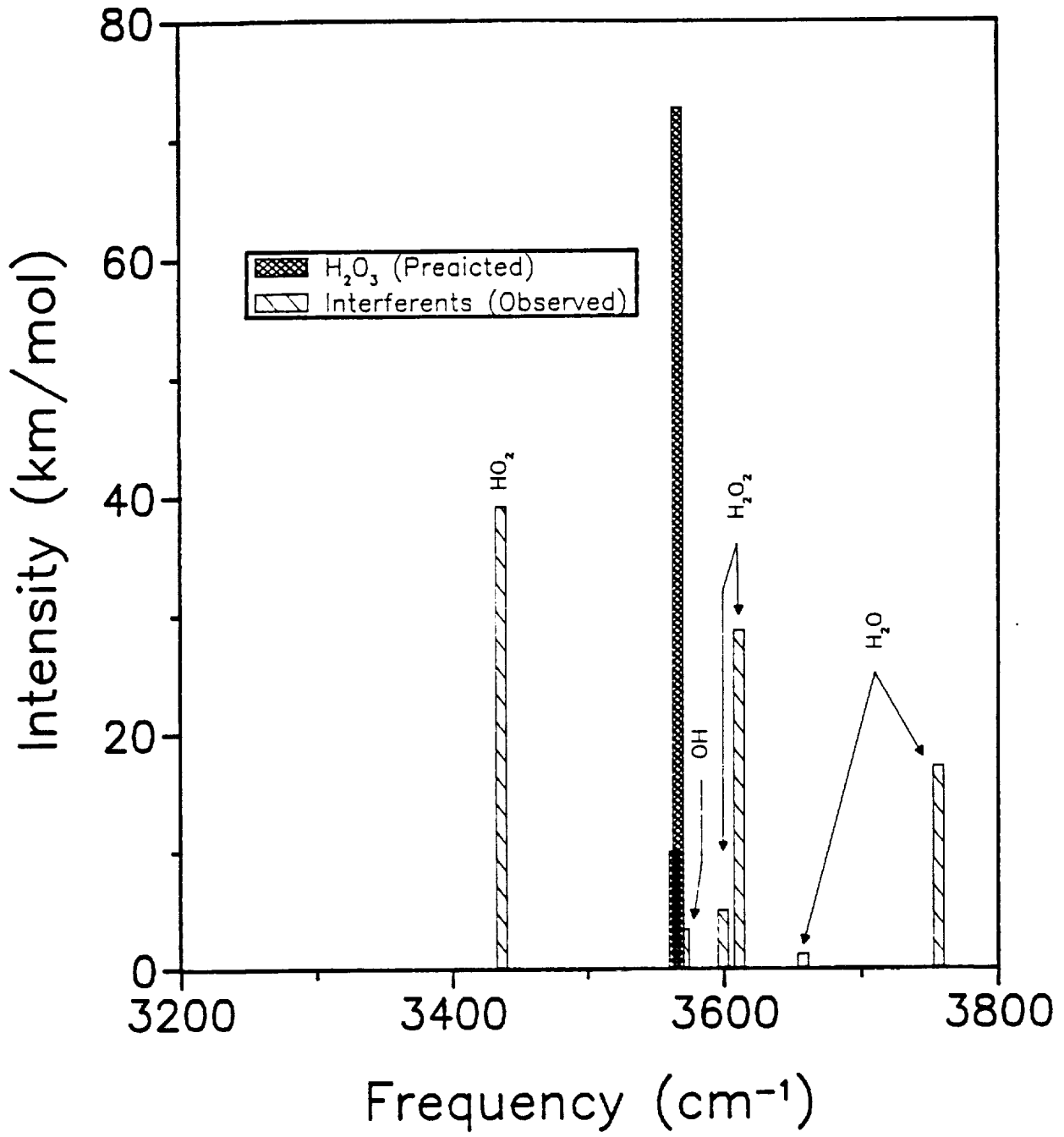


Figure 2 - Jackels

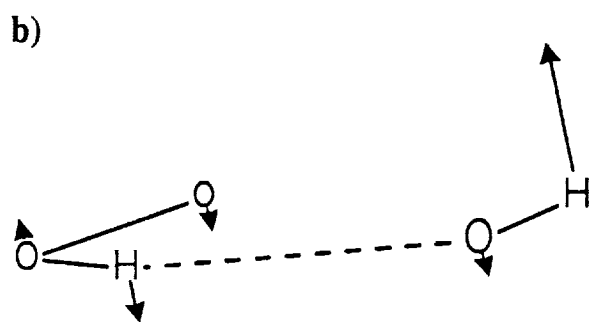
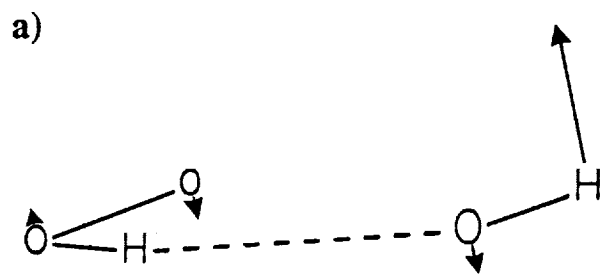
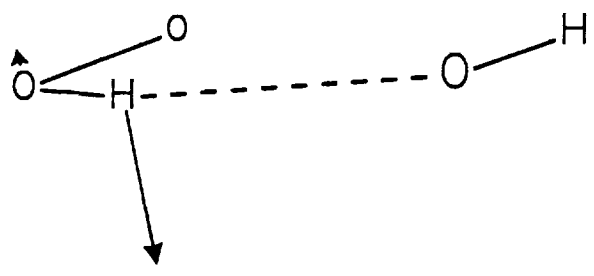


Figure 3 - Jackels

a)



b)

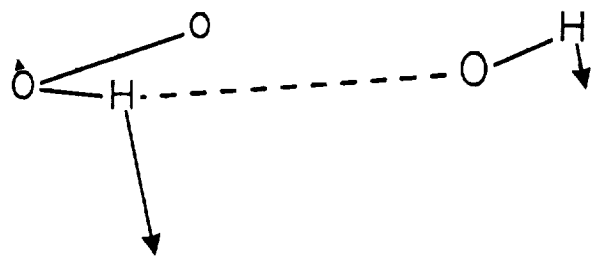


Figure 4 - Jackels

